Molecular Vision 2017; 23:242-250 <http://www.molvis.org/molvis/v23/242>
Received 20 November 2016 | Accepted 12 April 2017 | Published 14 April 2017

Resolvin D1 inhibits inflammatory response in STZ-induced diabetic retinopathy rats: Possible involvement of NLRP3 inflammasome and NF-κB signaling pathway

Yizhou Yin,[1,2] Fei Chen,[1,2] Wenyan Wang,[1,2] Han Wang,[1,2] Xuedong Zhang[1,2]

[1]Department of Ophthalmology, the First Affiliated Hospital of Chongqing Medical University, Chongqing, China; [2]Chongqing Key Laboratory of Ophthalmology, Chongqing Eye Institute, Chongqing, China

Purpose: To investigate the effect of resolvin D1 (RvD1) on the Nod-like receptor family pyrin domain-containing (NLRP3) inflammasome and the nuclear factor-kappa beta (NF-κB) pathway in streptozotocin (STZ)-induced diabetic retinopathy in rats.

Methods: Ninety-six male rats were divided into four groups: control, STZ, RvD1, and vehicle. The rats with diabetic retinopathy induced by STZ in the RvD1 and vehicle groups were given an intravitreal injection of RvD1 (1,000 ng/kg) or the same dosage of vehicle, respectively. All rats were euthanized 7 days following treatment. Hematoxylin and eosin staining was used to observe the pathological changes in the retinal tissues. The location and expression of the NLRP3 inflammasome components, including NLRP3, caspase-associated recruitment domain (ASC), and caspase-1, in the retinas were detected using immunohistochemistry, real-time PCR, and western blot, respectively. Retinal homogenate of rats were collected for the detection of the downstream molecules interleukin 1 beta (IL-1β) and IL-18 of the NLRP3 inflammasome with enzyme-linked immunosorbent assay kits.

Results: The levels of NLRP3, ASC, cleaved caspase-1, IL-1β, and IL-18 were upregulated in the retinas of the STZ-induced diabetic rats; however, these changes were partially inhibited by the RvD1 treatment. Furthermore, the administration of RvD1 suppressed activation of NF-kB, which was upregulated in STZ-induced diabetic retinopathy.

Conclusions: RvD1 plays a protective role in STZ-induced diabetic retinopathy by inhibiting the level of activation of the NLRP3 inflammasome and associated cytokine production, suggesting targeting of this pathway might be an effective strategy in treatment of diabetic retinopathy.

Diabetic retinopathy (DR) is a common microvascular complication of diabetes, which is regarded as one of the main causes of preventable blindness worldwide [1]. It has been shown that nearly all patients with type 1 diabetes, and more than 60% of patients with type 2 diabetes with a history of diabetes suffer from DR at some point [2]. The number of Americans with DR will triple from 5.5 million in 2005 to 16.0 million in 2050, while the number of vision-threatened patients with DR will increase from 1.2 million in 2005 to 3.4 million in 2050 among patients 40 years old or older. Furthermore, patients with DR aged 65 years old or older will increase to an even greater extent [3].

The pathogenesis of DR is poorly understood, although many mechanisms have been postulated to contribute to DR, such as activation of the polyol pathway, accumulation of advanced glycation end products (AGEs), the hexosamine pathway, inflammation, and protein kinase C (PKC) activation [4]. Growing evidence has shown that a parainflammatory response, characterized by a chronic low level of inflammation and disorder of immune responses, plays a prominent role in the pathogenesis of DR [5]. Moreover, retinas from animals with diabetes express high levels of proinflammatory cytokines, such as interleukin 1 beta (IL-1β) and tumor necrosis factor alpha (TNF-α), which have been reported to be involved in inflammatory responses in DR [6]. Therefore, in the present study we focused on the role of anti-inflammatory therapies in inhibiting DR.

Pattern-recognition receptors (PRRs) belong to the innate immune system and are responsible for recognizing pathogen-associated molecular patterns (PAMPs) of pathogenic microorganisms, followed by activation of innate and adaptive immune responses. Nod-like receptor family pyrin domain-containing protein (NLRP) is assembled by PRRs and is involved in the development of chronic inflammatory responses [7]. The NLRP3 inflammasome (as the most widely studied inflammasome) comprises NLRP3, apoptosis-associated speck-like protein containing a caspase-associated recruitment domain (ASC), and caspase-1 [8]. NLRP3 interacts with ASC to activate caspase-1, and once activated, the

Correspondence to: Xuedong Zhang, Department of Ophthalmology, the First Affiliated Hospital of Chongqing Medical University, No.1 You Yi Road, Yu Zhong District, Chongqing 400016, China; Phone: 0086-23-89012536. FAX: 0086-23-89012536; email: zxued@sina.com

NLRP3 inflammasome induces tissue injury through upregulation of the proinflammatory cytokines IL-18 and IL-1β [9]. A recent study implicated the inappropriate activation of the NLRP3 inflammasome in DR [10].

Resolvin D1 (RvD1) is derived from the w-3-polyunsaturated fatty acid (PUFA) docosahexaenoic acid (DHA) [11]. The therapeutic promise of RvD1 in chronic inflammatory diseases, such as rheumatoid arthritis, inflammatory bowel disease, and asthma, has been recognized [12]. However, the anti-inflammatory role of RvD1 in DR has not been elucidated. Therefore, we performed this study to investigate the effect and the possible mechanism of RvD1 in the retina and whether the NLRP3 inflammasome is a target for RvD1 in DR.

METHODS

Streptozotocin-induced diabetic model: Male Sprague–Dawley rats (200–250 g, 8 weeks old) were obtained from the Animal Care Committee of Chongqing Medical University (Chongqing, China), were raised in a specific pathogen-free room, and received a standard laboratory rat diet and water. Diabetes was induced with a single intraperitoneal injection of freshly prepared streptozotocin (STZ) solution in citrate buffer (pH 4.5) at 60 mg/kg in rats. The rats were considered to be diabetic with non-fasting blood glucose 250 mg/dl or greater after 1 week. Diabetic rats were raised for 12 weeks with a regular diet and unlimited water. All animal protocols were approved by the Ethics Committee of Chongqing Medical University and in accordance with the Association for Research in Vision and Ophthalmology (ARVO) Statement for the Use of Animals in Ophthalmic and Vision Research.

STZ-treated rats with intravitreal injection of RvD1: Ninety-six rats were included in this study and randomly assigned to four groups: the control (n = 26), STZ (n = 26), RvD1 (n = 22), and vehicle group (n = 22). All animals, except those in the control group, were STZ-treated rats. The rats in the RvD1 group were given an intravitreal injection of RvD1 (1000 ng/kg) using sterile syringes fitted with a 30-gauge needle containing 5 µl of reconstituted RvD1 solution. Rats in the vehicle group were given an intravitreal injection of the same amount of saline and ethanol. All animals were euthanized 7 days after the respective treatment. . The rats were deeply anaesthetized by an intraperitoneal injection of 10% chloral hydrate (300 mg/kg).

Measurement of blood–retinal barrier permeability: The blood–retinal barrier (BRB) permeability was performed using the Evans blue (EB) technique. The rats were deeply anaesthetized with an intraperitoneal injection of 10% chloral hydrate (300 mg/kg) and then injected with EB dye solution dissolved in low concentration saline at a concentration of 30 mg/ml through the tail vein, at a dosage of 45 mg/kg. After 120 min, the rats were perfused with PBS (1X; 137 mM NaCl, 2.7 mM KCl, 4.3 mM Na_2HPO_4, 1.4 mM KH_2PO_4, pH7.4) followed by 1% paraformaldehyde via the left ventricle. After dissecting and drying, the weight of the retina was measured. Each retina was incubated in 200 µl formamide overnight at 70 °C and centrifuged at 20,000 ×g for 60 min. Supernatant retinal extracts were tested spectrophotometrically at 620 nm and 740 nm.

Histological analysis: The eyeballs were harvested and fixed via immersion in 4% paraformaldehyde for 24 h. The 10% buffered formalin-fixed retina tissue was embedded in paraffin and sectioned at 5 µm. Following staining with hematoxylin and eosin (H&E), the paraffin sections were observed and photographed with a fluorescence microscope (. Leica, Bannockburn, IL, DM6000).

Immunohistochemistry: The sections were washed four times for 5 min in PBS following deparaffinization and antigen retrieval. The slides were then blocked with goat serum for 30 min. All sections were subsequently incubated with anti-NLRP3 antibody (1:200 dilution, Santa Cruz Biotechnology, Santa Cruz, CA), anti-ASC antibody (1:200 dilution, Santa Cruz Biotechnology), and anti-caspase-1 antibody (1:200 dilution, Santa Cruz Biotechnology) at 4 °C overnight, followed by incubation with goat anti-rabbit biotinylated antibody (ZSGB-Bio, Beijing, China) at room temperature. Staining was developed with diaminobenzidine (DAB) and counterstained with hematoxylin. Sections incubated in PBS were used as negative controls. Three sections per eye were selected, with four rats in each group. Retinal images were obtained at the same distance from the optic nerve. Images of the immunohistochemically stained tissue sections were collected using an Olympus BX60 microscope (Olympus Optical Co Ltd, Tokyo, Japan).

mRNA expression detected with real-time PCR: Total mRNA was extracted from the retinal samples with TRIzol Reagent (Life Technologies, Grand Island, NY) according to the manufacturer's protocol. Quantitative PCR was performed using an Applied Biosystems 7500 Fast Real-Time PCR System (Foster City, CA). PCR primers employed were as follows: NLRP3, 5′-CCA GGG CTC TGT TCA TTG-3′ (forward) and 5′-CCT TGG CTT TCA CTT CG-3′ (reverse); ASC, 5′-CCC ATA GAC CTC ACT GAT AAA C-3′ (forward) and 5′-AGA GCA TCC AGC AAA CCA-3′ (reverse); caspase-1, 5′-AGG AGG GAA TAT GTG GG-3′ (forward) and 5′-AAC CTT GGG CTT GTC TT-3′ (reverse); IL-1β, 5′-CCT TGT GCA AGT GTC TGA AG-3′ (forward) and 5′-GGG CTT GGA AGC AAT

CCT TA-3′ (reverse); IL-18, 5′-CGC AGT AAT ACG GAG CAT AAA TGA C-3′ (forward) and 5′-GGT AGA CAT CCT TCC ATC CTT CAC-3′ (reverse); and β-actin, 5′-AGG GAA ATC GTG CGT GAC-3′ (forward) and 5′-CGC TCA TTG CCG ATA GTG-3′ (reverse). Cycling conditions were 30 s of polymerase activation at 95 °C, followed by 40 cycles at 95 °C for 5 s and at 60 °C for 34 s. The data were analyzed using the $2^{-\Delta\Delta CT}$ method.

Protein expression measured with western blot: Retinas were homogenized in ice-cold radioimmunoprecipitation assay (RIPA) lysis buffer containing protease inhibitors or a Nuclear and Cytoplasmic Protein Extraction Kit (Beyotime, Haimen, China) and centrifuged at 12,000 ×*g* for 20 min at 4 °C. Protein samples were loaded on a Tris glycine gel, separated with 10% sodium dodecyl sulfate–polyacrylamide gel electrophoresis (SDS–PAGE), and transferred onto polyvinylidene difluoride membranes. The membranes were then blocked with 5% skim milk for 2 h at 37 °C and incubated overnight at 4 °C with the following antibodies: anti-NLRP3 antibody (Santa Cruz Biotechnology) at 1:200 dilution, anti-ASC antibody (Santa Cruz Biotechnology) at 1:200 dilution, anti-caspase-1 antibody (Proteintech, Wuhan, China) at 1:500 dilution, antibodies to IκBα (Santa Cruz Biotechnology) at 1:500 dilution, nuclear factor-kappa B (NF-κB) p65 (Santa Cruz Biotechnology) at 1:200 dilution, and p-NF-kB p65 (Abcam, Cambridge, UK) at 1:700 dilution. After being washed with Tris-buffered saline with Tween 20 (TBS-T), the membranes were then incubated with goat anti-rabbit horseradish peroxidase-conjugated secondary antibodies (Sigma, St. Louis, MO) for 1 h at 1:5,000 dilution at room temperature. The immunoreactive bands were visualized using an enhanced chemiluminescence method and quantified with densitometry analysis (Quantity One, Hercules, CA). GAPDH was used as a loading control.

ELISA: Retinas were isolated and homogenized in 150 µl of RIPA lysis buffer, supplemented with 1% protease inhibitors followed by centrifugation at 15,000 ×g for 25 min at 4 °C. The levels of IL-1β and IL-18 were measured in the extracted supernatant using commercial kits. The kits used for the measurement of cytokines were as follows: IL-1β (eBioscience, Santa Clara, CA, Ref: BMS630, Lot: 87,225,015) and IL-18 (Novex, Invitrogen, Camarillo, CA, Ref: KRC2341, Lot: 130,401/A).

Statistical analysis: Data were expressed as mean ± standard deviation (SD). Statistical comparisons among the groups were performed using one-way ANOVA (ANOVA) followed by the Student–Newman–Keuls (SNK) test for multiple comparisons. A p value of less than 0.05 was considered statistically significant. Statistical calculations were performed using SPSS Software 19.0 (SPSS, Inc., Chicago, IL).

RESULTS

Observation of morphology in the retinas of STZ-treated rats: H&E staining showed a homogenous surface of the retina with the ganglion cells arranged in a monolayer, and regular arrangement of cells at the inner and outer nuclear layers in the control group (Figure 1A). Twelve weeks after the STZ treatment, we observed disruption of the retinal structures, and the inner and outer nuclear layers appeared to be disordered (Figure 1B,C). The rats in the RvD1 group showed improvements in the distribution of the inner and outer nuclear layers compared with the STZ group (Figure 1D). In addition, as shown in Figure 1E, the permeability of the BRB in the STZ group was statistically significantly increased 2.4-fold compared with the controls ($p<0.01$).

RvD1 reduced NLRP3 inflammasome expression in the retinas of the STZ-treated rats: Immunohistochemical results showed that NLRP3, ASC, and caspase-1 were specifically located in the ganglion cell layer and the inner and outer nuclear layers (Figure 2A). The number of cells expressing NLRP3, ASC, and caspase-1 was remarkably increased in the STZ group ($p<0.001$) but decreased in the RvD1 group compared with the STZ group (Figure 2B; $p<0.01$). Compared with the control group, the mRNA levels of NLRP3, ASC, and caspase-1 were statistically significantly increased in the STZ group ($p<0.05$), which were inhibited by RvD1 administration as seen in Figure 2C ($p<0.05$).

In addition, as shown in Figure 2D–G intravitreal RvD1 administration statistically significantly inhibited the protein expression of NLRP3, ASC, and cleaved caspase-1 compared with the STZ group ($p<0.05$). Nevertheless, we did not observe any statistically significant difference between the STZ and vehicle groups.

RvD1 administration inhibited the expression of IL-1β and IL-18 through suppression of NLRP3 inflammasome activation: To investigate the changes in the downstream molecules mature IL-1β and IL-18 of NLRP3 inflammasome activation, we detected the levels with enzyme-linked immunosorbent assay (ELISA). As shown in Figure 3A,B, the treatment with STZ statistically significantly increased the expression of IL-1β and IL-18 (both $p<0.001$), while treatment with RvD1 showed a statistically significant reduction in the protein levels of IL-1β and IL-18 compared with the STZ group ($p<0.01$ and $p<0.001$, respectively). Meanwhile, consistent with the ELISA findings, the mRNA levels of IL-1β and IL-18 were decreased in the RvD1 group (Figure 3C,D).

RvD1 alleviated NF-kB activation in the retinas of the STZ-treated rats: Given the importance of NF-κB in the transcription of the cytokines in the NLRP3 inflammasome, we used western blotting to analyze protein expression. As seen in Figure 4, the levels of NF-κB phosphorylation (Figure 4A,B) and degradation of IκBα (Figure 4C,D) in the rats with STZ-induced DR were markedly increased (both $p<0.05$), whereas RvD1 suppressed the expression of NF-κB phosphorylation and decreased IκBα (both $p<0.05$).

DISCUSSION

In this study, we observed pathological morphology of the retina in STZ-induced retinopathy and the breakdown of the BRB, which contributes to the development of DR, resulting in hemorrhage, edema, and retinal detachment [13]. In addition, we found increased expression of the NLRP3 inflammasomes, including NLRP3, ASC, caspase-1, and its downstream inflammatory molecules, as well as the activation of NF-κB in diabetic retinas. In the present study, we also demonstrated that the upregulation of the NLRP3 inflammasome and the NF-κB pathway in diabetic rats was attenuated after treatment with RvD1. These findings indicate that RvD1 may inhibit the NLRP3 inflammasome and the NF-κB signaling pathway and may contribute to attenuation of the early stage of DR.

The disruption of the BRB occurs in the early stage of STZ-treated retinopathy [14]. Diabetic-induced endothelial dysfunction, leukostasis, and inflammation play an important role in the pathogenesis of DR, accounting for the initial change in BRB damage [15]. IL-1β increases vascular permeability via NF-κB activation, leukocyte adhesion, and retinal capillary cell apoptosis [16]. In the present study, the permeability of the BRB in the STZ group was statistically significantly increased after 3 months, which may be accounted for by the actions of IL-1β and IL-18. In addition,

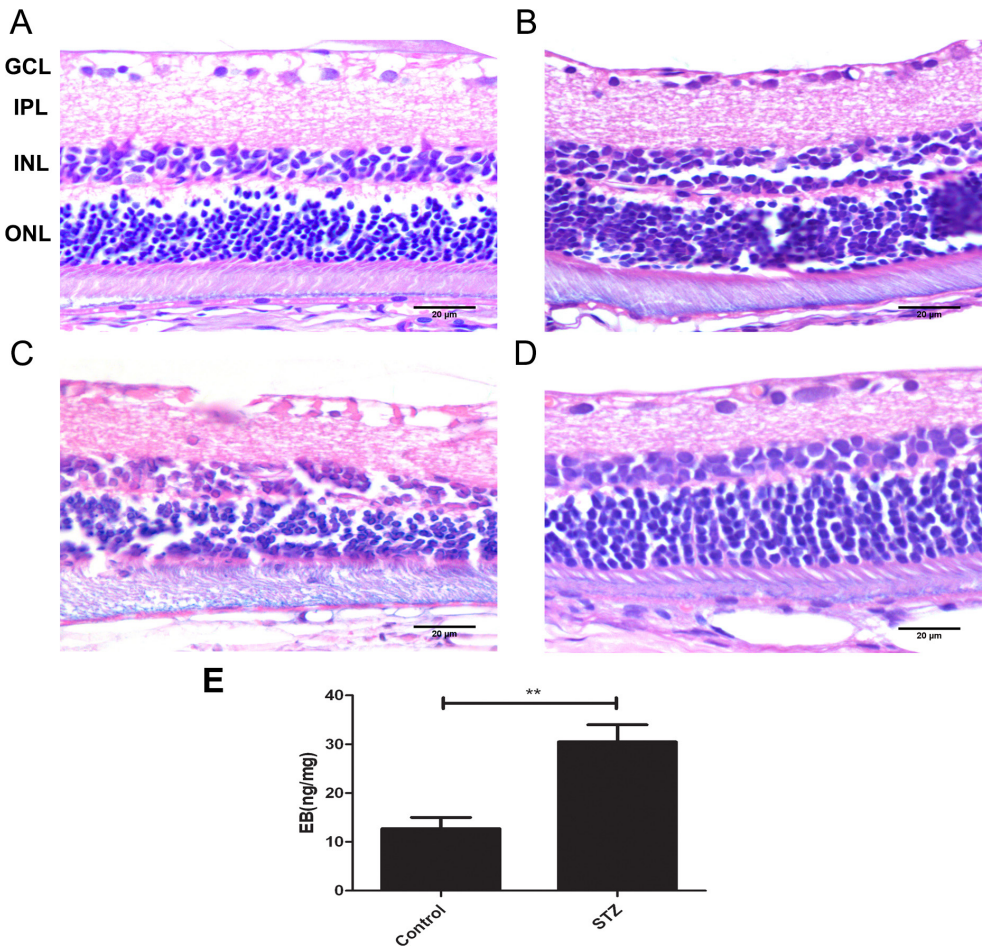

Figure 1. Pathological observation in retinas of rats with STZ-induced DR. Representative photomicrographs of hematoxylin and eosin (H&E) staining of retinopathy. Scale bars = 20 μm. **A**: The control group (n = 4) showed a homogenous surface. The inner and outer nuclear layers were all regularly arranged. **B**: In the group treated with streptozotocin (STZ; n = 4), morphological changes in the rats with diabetic retinography (DR) were observed, including disruption and irregular arrangement of cells in the outer and inner nuclear layers. **C**: The vehicle group (n = 4) showed a disordered structure and irregular cells in the outer and inner nuclear layers. **D**: The resolvin D1 (RvD1) group (n = 4) illustrated that the inner and outer nuclear layers were tighter and the cells were more regular. Original magnification = 400X. GCL = ganglion cell layer; INL = inner nuclear layer; ONL = outer nuclear layer. **E**: The permeability of the blood–retinal barrier was tested with the Evans blue permeation assay. The leakage in the retinas of the diabetic rats after 3 months was statistically significantly higher than that in the control group. **$p<0.01$. Values are expressed as mean ± standard deviation (SD); n = 4 experiments.

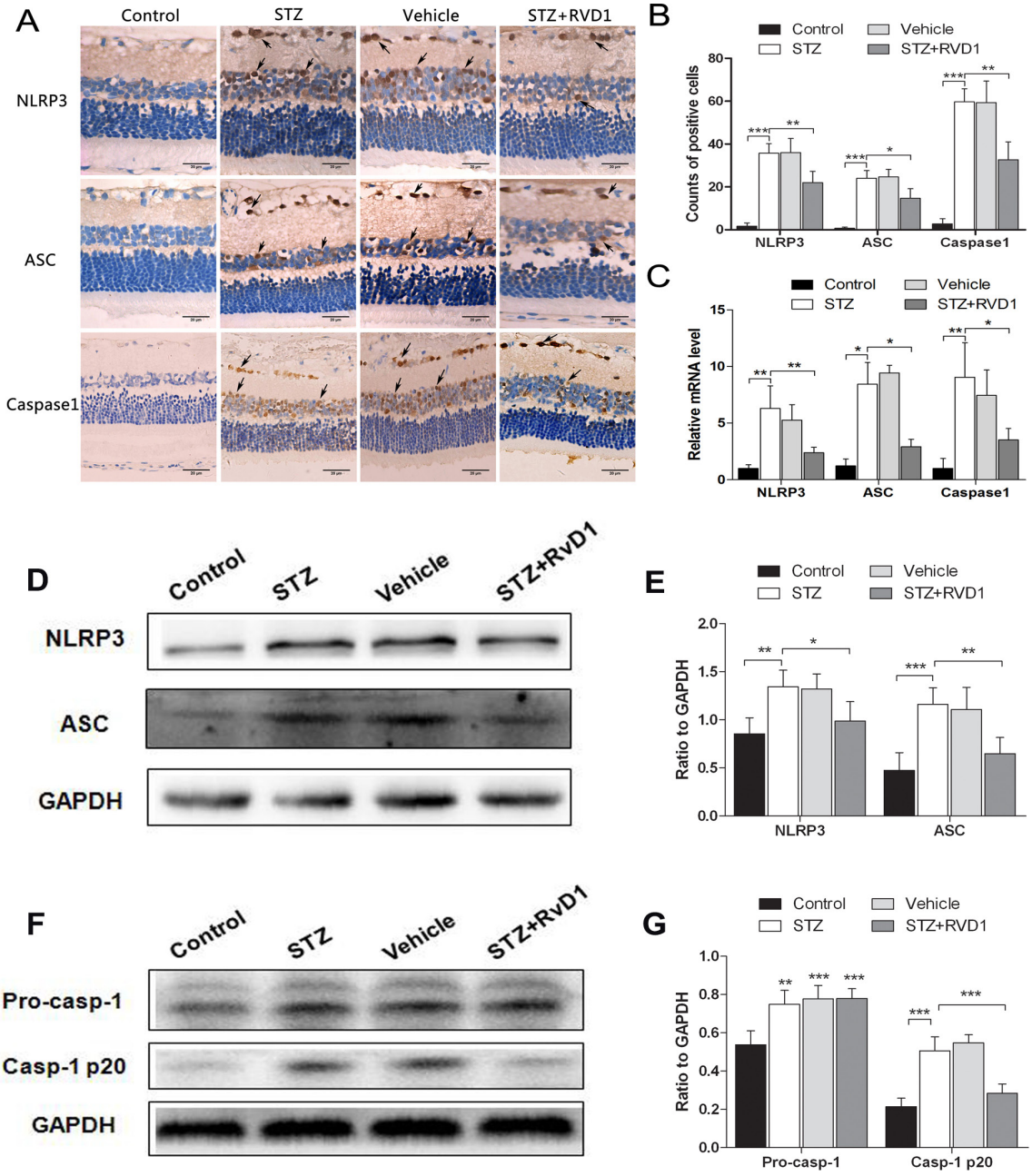

Figure 2. Intravitreal injection of RvD1 inhibited NLRP3, ASC, and caspase-1 expressions in rat retinas. **A**: Representative immunohistochemical images of the expression of Nod-like receptor family pyrin domain-containing (NLRP3), caspase-associated recruitment domain (ASC), and caspase-1 in the retina. Immunohistochemical staining shows the location of NLRP3, ASC, and caspase-1 expression in the ganglion cell layer (GCL) and the inner nuclear layer (INL). The number of positive cells expressing NLRP3, ASC, and caspase-1 were remarkably increased in the group treated with streptozotocin (STZ) compared with the control group. Intravitreal injection of resolvin D1 (RvD1) decreased the expression of NLRP3, ASC, and caspase-1 compared with the STZ-treated group. The brown granules marked with arrows represent corresponding specific staining (400X). Scale bar = 20 μm (n = 4). **B**: Quantification of the positive cells in the retinas. Three sections per eye were averaged. RvD1 decreased the number of positive cells in the STZ-treated group compared with the RvD1 group. **C**: RvD1 treatment decreased the mRNA expression of NLRP3, ASC, and caspase-1 in the retinas of the STZ-treated rats. **D**: Representative western blot showing the protein expression of NLRP3 and ASC in the rat retinas. GAPDH was used as a loading control. **E**: Column diagrams representing the ratio of the scanned immunoblots of NLRP3 and ASC to that of GAPDH. **F**: Representative western blot showing the protein expression of pro-caspase-1 and caspase-1 p20 in rat retinas. **G**: Column diagrams representing the ratio of the scanned immunoblots of pro-caspase-1 and caspase-1 p20 to that of GAPDH. Data are expressed as mean ± standard deviation (SD). *p<0.05, ** p<0.01, *** p<0.001. n = 6 experiments.

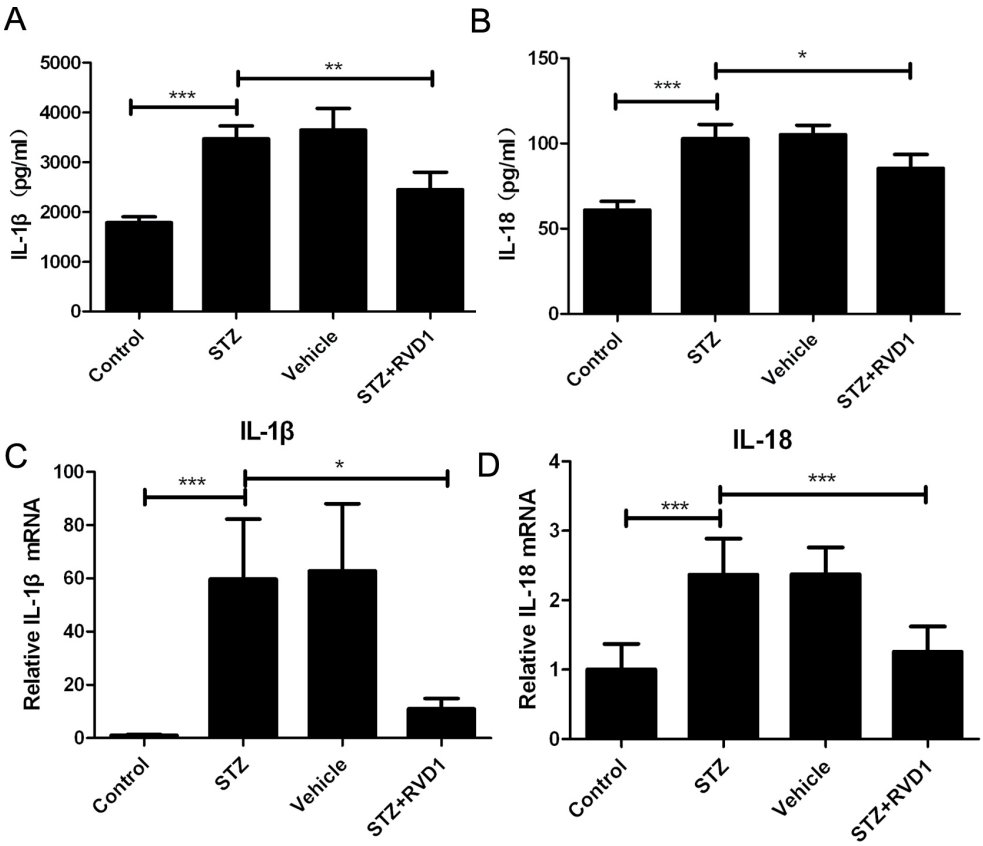

Figure 3. Effect of RvD1 on the expression of IL-1β and IL-18 in STZ-treated rats. **A**: Retinal expression of interleukin-1 beta (IL-1β) was increased in the streptozotocin (STZ)-treated group compared with the control groups but decreased after injection of resolvin D1 (RvD1). **B**: The protein expression of IL-18 was statistically significantly upregulated in the retinas of the STZ group and the vehicle group compared with the control group and reduced in the RvD1 group. **C**: The mRNA expression of IL-1β in the retina was increased in the STZ and vehicle groups compared with the control group while reduced by injection of RvD1 in the RvD1 group. **D**: The mRNA expression of IL-18 in the retina was markedly increased in the STZ group and the vehicle group compared with the control group. However, the level of mRNA expression was decreased by intravitreal injection of RvD1. * $p<0.05$, ** $p<0.01$, *** $p<0.001$. Values are expressed as mean ± standard deviation (SD); n = 6 experiments.

we observed disruption of the inner and outer retinal nuclear layers in diabetic rats.

Hyperglycemia and other stresses lead to a series of inflammatory mediators in diabetes, which trigger parainflammatory responses that might cause abnormal leukocyte–endothelial interactions and, ultimately, retinal microvascular damage [17]. Chronic inflammation is one of the key triggers in the pathogenesis of DR, and a reduction in inflammation has been reported to alleviate the development and progression of DR [18]. For this reason, we aimed to prevent chronic inflammation in a model of DR. Studies have reported that NLRP plays an important role in the development of chronic inflammatory responses through IL-1β and IL-18 secretion. Activation of the NLRP3 inflammasome has been demonstrated in a wide variety of diseases, including asbestosis, Alzheimer disease, atherosclerosis, and gout [19-21]. An emerging role of the NLRP3 inflammasome in the development of diabetic nephropathy suggested the involvement of NLNRP3 in renal inflammation [22]. In addition, Shi et al. [23] observed that the NLRP3 inflammasome could be activated in ARPE-19 cells under high glucose stress in vitro. In this study, we also found that the NLRP3 inflammasome pathway was involved in the development of DR in a type 1 diabetic rat model, which further confirmed the role of the NLRP3 inflammasome in DR.

RvD1, derived from the essential omega-3 fatty acid docosahexaenoic acid (DHA), has been shown to have a protective role in several diseases, including hepatic ischemia/reperfusion injury [24], adjuvant-induced arthritis [25], peritonitis [26], and uveitis [27]. However, whether RvD1 can regulate the NLRP3 inflammasome and prevent the progression of DR is unclear. Because o-3-polyunsaturated fatty acids have been reported to protect against retinopathy and reduce angiogenesis [28], we speculate that RvD1 may exert its anti-inflammatory effects by targeting the NLRP3 inflammasome. Our results showed that RvD1 inhibited the expression of the NLRP3 inflammasome and its downstream signaling pathway in diabetic retinas, which promoted the resolution of inflammation in DR. Therefore, we concluded that RvD1 might be a potent inhibitor of the NLRP3 inflammasome signaling pathway, which could maintain potent

anti-inflammatory properties in a diabetic rat model of chronic inflammation.

Caspases, categorized as either proinflammatory or proapoptotic factors, can lead to inflammation or cell death. Caspase-1, activated by the NLRP3 inflammasome, mediates cytokines such as IL-1β [29]. Activated caspase-1 processes pro-IL-1β to a mature form and subsequently induces proinflammatory cytokine release and inflammation [30]. IL-1β is a potent proinflammatory mediator, and maturation and release are mediated by inflammasome activation. Secretion of the inflammatory cytokines IL-1β and IL-18 play a pivotal role in the development of DR and are critically regulated by the NLPR3 inflammasome [31,32]. Consistent with previous studies, the present data revealed that levels of the inflammatory cytokines IL-1β and IL-18 were elevated in the STZ-induced DR model but decreased with the administration of RvD1. Collectively, RvD1 downregulated the expression of IL-1β and IL-18, most likely through the inhibition of the NLRP3 inflammasome signaling pathway.

NF-κB, a ubiquitously expressed transcription factor that regulates many inflammatory cytokines, has been shown to regulate DR. Under physiologic conditions, NF-κB is silenced by its inhibitor, IkB. Persistent activation of NF-κB initiates an increase in inflammatory cytokines during the inflammatory response that regulates cell proliferation, invasion, apoptosis, and metastasis [33]. It is known that the activation of NF-κB is involved in the NLRP3 inflammasome [34]. Our results showed enhanced phosphorylation of NF-κB and degradation of IκBα and increased inflammatory cytokine production in STZ-treated rats retinas compared with the control group. In accordance with previous studies showing that RvD1 regulates the phosphorylation of NF-κB [35], the present results revealed that RvD1 treatment inactivated the NF-κB-related signaling pathway via inhibition of NF-κB phosphorylation and blockade of the degradation of IκBα, suggesting an inhibitory effect of RvD1 on NF-κB activity and subsequent inflammatory responses in DR.

In conclusion, we found a suppressive action of RvD1 on the activation of NLRP3 inflammasome-associated component proteins, including NLRP3, ASC, caspase-1, and NF-κB activation. We also found an inhibitory role of RvD1 relative to the production of IL-1β and IL-18. The present study results indicate that the NLRP3 inflammasome contributes

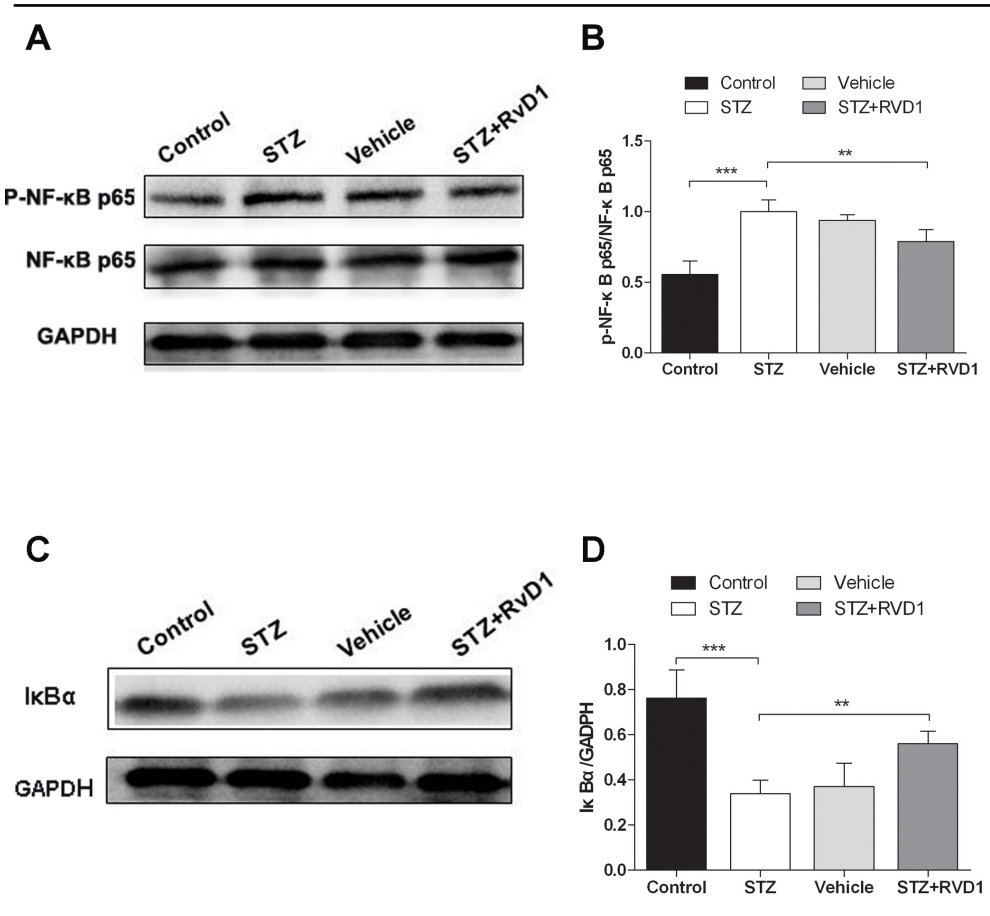

Figure 4. RvD1 alleviated the phosphorylation of NF-κB and degradation of IκBα in the retinas of STZ-treated rats. **A**: Western blot analysis of the nuclear factor kappa beta (NF-κB) phosphorylation in the retinas of diabetic rats with or without the treatment of resolvin D1 (RvD1). **B**: The levels of NF-κB phosphorylation were increased in the retinas of diabetic rats compared with the control group, while the increase was statistically significantly blocked in the RvD1 group. **C**: Western blot analysis of the degradation of IκBα in the retinas of diabetic rats with or without the treatment of RvD1. **D**: Enhanced degradation of IκBα in the retinas of diabetic rats was blocked by RvD1. Each column denotes the mean ± standard deviation (SD); n = 6. * p<0.05, **p<0.01, *** p<0.001.

to the pathogenesis of STZ-induced DR, and RvD1 may be an alternative therapeutic agent for DR.

ACKNOWLEDGMENTS

This study was supported by funds from National Natural Science Foundation of China (81,371,043), the special fund of Chongqing Key Laboratory of Ophthalmology (CSTC, 2008CA5003) and National Key Clinical Specialties Construction Program of China. The authors would like to express their thanks to M r. Peizeng Yang and Mrs. Chaokui Wang for their kind advice.

REFERENCES

1. Yau JW, Rogers SL, Kawasaki R, Lamoureux EL. Global Prevalence and Major Risk Factors of Diabetic Retinopathy. Diabetes Care 2012; 35:556-64. [PMID: 22301125].
2. Karadayi K, Top C, Gülecek O. The relationship between soluble L-selction and development of diabetic retinopathy. Ocular Immunology and Inflammation 2003,Vol,II,No.2,pp,123–129.
3. Saaddine JB, Honeycutt AA, Narayan KM, Zhang X, Klein R, Boyle JP. Projection of diabetic retinopathy and other major eye diseases among people with diabetes mellitus: United States, 2005–2050. Arch Ophthalmol 2008; 126:1740-7. [PMID: 19064858].
4. Wu Y, Tang L, Chen B. Oxidative stress: implications for the development of diabetic retinopathy and antioxidant therapeutic perspectives. Oxid Med Cell Longev 2014; •••:752387-[PMID: 25180070].
5. Antonetti DA, Barber AJ, Bronson SK, Freeman WM, Gardner TW, Jefferson LS. Diabetic retinopathy: seeing beyond glucose-induced microvascular disease. Diabetes 2006; 55:2401-11. [PMID: 16936187].
6. Tang J, Kern TS. Inflammation in diabetic retinopathy. Prog Retin Eye Res 2011; 30:343-58. [PMID: 21635964].
7. Schroder K, Tschopp J. The inflammasomes. Cell 2010; 140:821-32. [PMID: 20303873].
8. Mori MA, Bezy O, Kahn CR. Metabolic syndrome: is Nlrp3 inflammasome a trigger or a target of insulin resistance? Circ Res 2011; 108:1160-2. [PMID: 21566220].
9. Strowig T, Henao-Mejia J, Elinav E, Flavell R. Inflammasomes in health and disease. Nature 2012; 481:278-86. [PMID: 22258606].
10. Ward R, Ergul A. Relationship of endothelin-1 and NLRP3 inflammasome activation in HT22 hippocampal cells in diabetes. Life Sci 2016; 159:97-103. [PMID: 26883974].
11. Serhan CN, Chiang N, Van Dyke TE. Resolving inflammation: dual antiinflammatory and pro-resolution lipid mediators. Nat Rev Immunol 2008; 8:349-61. [PMID: 18437155].
12. Calder PC. Marine omega-3 fatty acids and inflammatory processes: Effects, mechanisms and clinical relevance. Biochim Biophys Acta 2015; 1851:469-84. [PMID: 25149823].
13. Xu H, Cai M. Effect of the blockade of the IL-23-Th17-IL-17A pathway on streptozotocin-induced diabetic retinopathy in rats. Graefes Arch Clin Exp Ophthalmol 2015; 253:1485-92. [PMID: 25371107].
14. Kaya A, Kar T, Aksoy Y, Özalper V, Başbuğ B. Insulin analogues may accelerate progression of diabetic retinopathy after impairment of inner blood-retinal barrier. Med Hypotheses 2013; 81:1012-4. [PMID: 24090664].
15. Cunha-Vaz J, Ribeiro L, Lobo C. Phenotypes and biomarkers of diabetic retinopathy. Prog Retin Eye Res 2014; 41:90-111. [PMID: 24680929].
16. Vincent JA, Mohr S. Inhibition of caspase-1/interleukin-1beta signaling prevents degeneration of retinal capillaries in diabetes and galactosemia. Diabetes 2007; 56:224-30. [PMID: 17192486].
17. Cheung N, Mitchell P, Wong TY. Diabetic retinopathy. Lancet 2010; 376:124-36. [PMID: 20580421].
18. Tarr JM, Kaul K, Chopra M, Kohner EM, Chibber R. Pathophysiology of diabetic retinopathy. ISRN Ophthalmol 2013; •••:343560-[PMID: 24563789].
19. Dostert C, Pétrilli V, Van Bruggen R, Steele C, Mossman BT, Tschopp J. Innate immune activation through Nalp3 inflammasome sensing of asbestos and silica. Science 2008; 320:674-7. [PMID: 18403674].
20. Martinon F, Pétrilli V, Mayor A, Tardivel A, Tschopp J. Gout-associated uric acid crystals activate the NALP3 inflammasome. Nature 2006; 440:237-41. [PMID: 16407889].
21. Duewell P, Kono H, Rayner KJ, Sirois CM. NLRP3 inflammasomes are required for atherogenesis and activated by cholesterol crystals that form early in disease. Nature 2010; 464:1357-61. [PMID: 20428172].
22. Qiu YY, Tang LQ. Roles of the NLRP3 inflammasomes in the pathogenesis of diabetic nephropathy. Pharmacol Res 2016; 114:251-[PMID: 27826011].
23. Shi H, Zhang Z, Wang X, Li RI, Hou W, Bi W, Zhang X. Inhibition of autophagy induces IL-1b release from ARPE-19 cells via ROS mediated NLRP3 inflammasome activation under high glucose stress. Biochem Biophys Res Commun 2015; 463:1071-6. [PMID: 26102024].
24. Zhang T, Shu HH, Chang L, Ye F, Xu KQ, Huang WQ. Resolvin D1 protects against hepatic ischemia/reperfusion injury in rats. Int Immunopharmacol 2015; 28:322-7. [PMID: 26118631].
25. Lima-Garcia JF, Dutra RC, da Silva K, Motta EM, Campos MM, Calixto JB. The precursor of resolvin D series and aspirin-triggered resolvin D1 display anti-hyperalgesic properties in adjuvant-induced arthritis in rats. Br J Pharmacol 2011; 164:278-93. [PMID: 21418187].
26. Tang Y, Zhang MJ, Hellmann J, Kosuri M, Bhatnagar A, Spite M. Proresolution therapy for the treatment of delayed healing of diabetic wounds. Diabetes 2013; 62:618-27. [PMID: 23043160].

27. Settimio R, Clara DF, Franca F, Francesca S, Michele D. Resolvin D1 reduces the immunoinflammatory response of the rat eye following uveitis. Mediators Inflamm 2012; •••:318621-[PMID: 23304060].

28. Connor KM, SanGiovanni JP, Lofqvist C, Aderman CM, Chen J, Higuchi A, Hong S, Pravda EA, Majchrzak S, Carper D, Hellstrom A, Kang JX, Chew EY, Salem N Jr, Serhan CN, Smith LE. Increased dietary intake of omega-3-polyunsaturated fatty acids reduces pathological retinal angiogenesis. Nat Med 2007; 13:868-73. [PMID: 17589522].

29. Martinon F, Burns K, Tschopp J. The inflammasome: a molecular platform triggering activation of inflammatory caspases and processing of proIL-beta. Mol Cell 2002; 10:417-26. [PMID: 12191486].

30. Devi TS, Lee I, Hüttemann M, Kumar A, Nantwi KD, Singh LP. TXNIP Links Innate host defense mechanisms to oxidative stress and inflammation in retinal Muller glia under chronic hyperglycemia: implications for diabetic retinopathy. Exp Diabetes Res 2012; •••:438238-[PMID: 22474421].

31. Dinarello CA. A clinical perspective of IL-1beta as the gatekeeper of inflammation. Eur J Immunol 2011; 41:1203-17. [PMID: 21523780].

32. Leemans JC, Cassel SL, Sutterwala FS. Sensing damage by the NLRP3 inflammasome. Immunol Rev 2011; 243:152-62. [PMID: 21884174].

33. Sethi G, Sung B, Aggarwal BB. Nuclear factor-KappaB activation: from bench to bedside. Exp Biol Med (Maywood) 2008; 233:21-31. [PMID: 18156302].

34. Shao A, Wu H, Hong Y, Tu S, Sun X, Wu Q, Zhao Q, Zhang J, Sheng J. Hydrogen-Rich Saline Attenuated Subarachnoid Hemorrhage-Induced Early Brain Injury in Rats by Suppressing Inflammatory Response: Possible Involvement of NF-κB Pathway and NLRP3 Inflammasome. Mol Neurobiol 2016; 53:3462-76. [PMID: 26091790].

35. Kaarniranta K, Salminen A. NF-kappaB signaling as a putative target for omega-3 metabolites in the prevention of age-related macular degeneration (AMD). Exp Gerontol 2009; 44:685-8. [PMID: 19751815].

Articles are provided courtesy of Emory University and the Zhongshan Ophthalmic Center, Sun Yat-sen University, P.R. China. The print version of this article was created on 14 April 2017. This reflects all typographical corrections and errata to the article through that date. Details of any changes may be found in the online version of the article.